KECK HIRES SPECTROSCOPY OF CANDIDATE POST T TAURI STARS

Eric J. Bubar

Department of Physics and Astronomy, Clemson University, Clemson, SC 29630-0978

`ebubar@clemson.edu`

Jeremy R. King

Department of Physics and Astronomy, Clemson University, Clemson, SC 29630-0978

`jking2@ces.clemson.edu`

David R. Soderblom

Space Telescope Science Institute, 3700 San Martin Drive, Baltimore, MD 21218

`soderblom@stsci.edu`

Constantine P. Deliyannis

Department of Astronomy, Indiana University, 727 East 3rd Street, Swain Hall West 319, Bloomington, IN 47405-7105

`con@athena.astro.indiana.edu`

and

Ann M. Boesgaard[1]

Institute for Astronomy, 2680 Woodlawn Drive, Honolulu, HI 96822

`boes@ifa.hawaii.edu`

ABSTRACT

We use high-signal-to-noise ($\sim$150-450), high resolution ($R\sim45,000$) Keck HIRES spectroscopy of 13 candidate post T Tauri stars to derive basic physical parameters, lithium abundances and radial velocities. We place our stars in the M_v-T_{eff} plane for use in determining approximate ages from pre-main sequence isochrones, and confirm these using three relative age indicators in our analysis: Li abundances, chromospheric emission and the kinematic U-V plane. Using the three age criteria we identify 5 stars (HIP 54529, HIP 62758, HIP 63322, HIP 74045, and HIP 104864) as probable post T Tauri stars with ages between 10 and 100 Myr. We confirm HIP 54529 as an SB2 and HIP 63322 as an SB1 star. We also examine irregular photometric variability of PTTs using the *HIPPARCOS* photometry annex. Two of our PTT stars exhibit near-IR excesses compared to Kurucz model flux; while recent work suggests classical T Tauri stars evince similar *JHK* excesses presumably indicative of non-photospheric (disk) emission, our results may be illusory artifacts of the chosen I-band normalization. Near-IR excesses we see in a literature-based sample of PTTs appear to be artifacts of previous spectral type-based T_{eff} values. Indeed, comparison of the homology of their observed and model photospheric SED's suggests that photometric temperatures are more reliable than temperatures based on spectral standards for the cooler temperature ranges of the stars in this sample. We conclude that our age oriented analysis is a robust means to select samples of nearby, young, isolated post T Tauri stars that otherwise masquerade as normal field stars.

Subject headings: stars: late type - stars: lithium - stars: post T Tauri

1.   INTRODUCTION

The evolution of young stars is becoming increasingly important given the renewed interest in planet formation driven by the continuing discovery of exoplanets (e.g.Butler et al. (2006)). The extremely young ($< 10^7$ yr) pre-main sequence precursors to stars like our own Sun, known as T Tauri stars, are believed to possess environments conducive to planetary formation. Auspiciously, T Tauri stars have distinct observational characteristics that make them relatively easy to identify. Such characteristics include, but are not limited to, strong infrared excesses, strong Hα emission, irregular variability and high surface lithium abundances (for a recent review of T Tauri stars refer to Petrov (2003) and references therein). By studying young stellar associations, T Tauri stars are fairly easily identifiable. However, the period of evolution (10^7 to 10^8 yrs) between the T Tauri and zero-age main-sequence phases remains ambiguous. The late-type stars in this age range, referred to as post T Tauri

stars (PTTs), are expected to have some degree of "intermediary characteristics" between T Tauri and main sequence stages (Herbig (1978)). Consequently, a post T Tauri star should possess, for example, relatively high measures of chromospheric emission and relatively high surface Li abundances compared to main sequence stars of comparable mass. It may seem that finding these stars should be relatively simple. By looking near regions of T Tauri stars, we should find that some have evolved into their post T Tauri stage. In fact, as Herbig (1978) noted nearly 30 years ago, there must be many times more post T Tauri stars than there are T Tauri stars. Yet studies of young stars which typically concentrate on regions of active star formation often fail to find the numbers of PTTs that are expected.

Several explanations that could resolve this apparent disparity are discussed in Soderblom et al. (1998), but here we will concentrate on their second solution: that PTTs exist, but are far from star-forming regions. To summarize their findings, Soderblom et al. (1998) showed HD98800 to be a unique PTT system. This system of four stars was determined to be a young ($\sim$10 Myr) post T Tauri group that is far from any region of active star formation. The orbital properties of the stars mean the system could not have been violently removed from its birthplace. It departed by a more gentle means, suggesting that it is possible that other post T Tauri candidates evolved similarly and now exist in isolated environments.

Most recently, post T Tauri search efforts have uncovered loose associations and moving groups that appear to be of post T Tauri age (the β Pictoris moving group, the TW Hydrae Association, the Tucana/Horologium Association, and the AB Doradus Moving Group)(Zuckerman & Song (2004) and references therein). In fact, HD98800 is now believed to be a member of just such a group (the TW Hydrae association). While it is beginning to appear that post T Tauri stars exist in associations, the sparseness of these groups and their relatively large spread throughout the sky makes their identification problematic. The salient question, then, is how to find these isolated PTTs in the field, away from any regions of star formation. Without a logical starting point, these stars simply cannot be found other than through serendipitous means. In this paper, though, we use an age-oriented definition drawing from the recommendations of Jensen (2001). For our purposes, we define a post T Tauri star as a young, low mass, pre-main sequence star with an age in the range from 10^7 to 10^8 years, where emergence of a stellar core at visible wavelengths is taken as an age of zero following the work of D'Antona & Mazzitelli (1997). This age-based definition is also useful by preventing incorrect classification of a weak-lined T Tauri (wTTS) or naked T Tauri (nTTS), which can have features comparable to a PTTs, but may be significantly younger.

The objects studied here are part of our ongoing survey of solar-type stars within 60pc based on low-resolution (R$\sim$2000) spectra mostly from KPNO Coude Feed. For the purpose

of follow-up high resolution spectroscopic programs, we flagged stars a) residing significantly above the *HIPPARCOS*-based main sequence and/or b) apparently evincing significant Ca II HK emission in raw 2-d spectra inspected by eye at the telescope as potential PTT candidates.

Here we present high-resolution echelle spectroscopy for 13 of these stars. We will derive qualitative age information from three diagnostics (Li abundance, chromospheric emission, and *UVW* kinematics) for use in assigning post T Tauri candidacy. We will also determine approximate ages from pre-main sequence isochrones and masses from pre-main sequence mass tracks, both taken from D'Antona & Mazzitelli (1997) (assuming solar metallicity). For completeness, we will also search for indications of irregular variability, examine infrared excesses, and present equivalent widths for the Hα feature: all characteristics noted by Herbig (1978) to be useful for identifying post T Tauri stars. We present our interpretations of these three features but choose not to include them in our age-oriented analysis as they typically decay on shorter timescales than our chosen indicators, making them less robust.

2. DATA AND ANALYSIS

2.1. *Observations and Reductions*

Spectroscopy of our objects was obtained on May 28 and 29, 2000 using the W.M. Keck I 10-m telescope (Table 1), the HIRES echelle spectrograph, and a Tektronix 2048×2048 CCD detector. The instrumental setup yielded a resolution of $R{\sim}45{,}000$ (3.2 pixel FWHM) and (incomplete) wavelength coverage from 4400 to 6800 Å. Standard reductions including bias correction, flat-fielding, scattered light correction, order extraction, and wavelength calibrations (with rms residuals of $\sim$0.002 Å) were carried out using standard routines in the echelle package of IRAF[1]. Measured per-pixel S/N values near the Li I λ6707 region ranged from 150-450 and are listed in Table 1. Sample spectra in the lithium region can be seen in Figure 1.

---

[1]IRAF is distributed by the National Optical Astronomy Observatories, which are operated by the Association of Universities for Research in Astronomy, Inc., under cooperative agreement with the National Science Foundation.

2.2. Basic Physical Parameters

Temperatures were determined from photometric calibrations of Ramírez & Meléndez (2005). Both B-V color indices from the Tycho catalog (Perryman & ESA 1997) and V-K_{2mass} indices (Cutri et al. 2003) were used to find effective temperatures. Errors for temperatures were found from the errors in the respective color indices and in the polynomial fits (Table 2 of Ramírez & Meléndez (2005)). A weighted mean was taken for input into Kurucz model atmospheres. Our sample, colors, temperatures and other data are compiled in Table 2.

Special methods had to be utilized for one of the stars in the sample (HIP 54529) as it was found to be a double-lined spectroscopic binary. Following the analysis of Boesgaard & Tripicco (1986), we performed a least squares fit to the ratio of equivalent widths of two Fe I absorption lines (W(6703)/W(6705)) versus effective temperature for the stars in our sample (Fig 2). We find the fit is given by the formula

$$\frac{W(6703)}{W6705} = 2.066 - 2.225(10^{-4})T_{eff}. \tag{1}$$

We used the equivalent widths of these lines in the primary and secondary components to determine their respective temperatures. Multiplicative correction factors to account for unequal continuum flux contributions from the components (as described in Boesgaard & Tripicco (1986)) were found to be approximately unity. We report here on the analysis for only the primary component. This technique was not applied to HIP 63322 as it was not a double-lined star. The double nature of this star was revealed by asymmetry in the cross-correlation peaks of our radial velocity analysis.

Our photometric temperatures can be compared to the spectroscopic values of Santos et al. (2004) for 6 stars in the sample (footnote 'a' of Table 2). We find that our temperatures for warmer stars tend to agree nicely with their spectroscopic estimates but become systematically cooler (by as much as 250 K at 4600 K) with declining temperatures. We suspect the spectroscopic T_{eff} values are afflicted by the effects of overexcitation seen in young cool dwarfs (Schuler et al. 2006). For this reason we have chosen to utilize photometric temperatures.

Use of Hipparcos parallaxes allowed us to calculate "physical" surface gravities using:

$$log\frac{g}{g_\odot} = log\frac{M}{M\odot} + 4log\frac{T_{eff}}{T_{eff,\odot}} + 0.4V_o + 0.4B.C. + 2log\pi + 0.12 \tag{2}$$

where M is the mass in solar masses (determined from the pre-main sequence mass tracks of D'Antona & Mazzitelli (1997)), V_o is the apparent magnitude and π is the parallax in

arcseconds. The surface gravity is given in Table 2. The average uncertainty for the surface gravity parameter was approximately 0.20 dex. We note that mass differences (as discussed in Section 3.2) from using tracks of Siess et al. (2000) and Baraffe et al. (1998) result in surface gravities that differ from our adopted ones by 0.01-0.17 dex when using the former and 0.01-0.18 dex when using the latter.

The microturbulence parameter was determined from calibrations of Allende Prieto et al. (2004). They derived a relationship for determining microturbulence as a function of effective temperature and surface gravity. The error in this parameter was determined by propagating the errors in effective temperature and $\log g$. The average error in the microturbulence was found to be 0.01 kms^{-1}. In order to examine the extent to which microturbulence would effect our lithium feature we performed lithium synthesis for microturbulent velocities spanning 1 kms$^-$1. We find this change to have very little effect on the lithium feature (≤ 0.01 dex).

Overall metallicities were kindly provided by R. Boone and are given in Table 2. These are derived based on χ^2 fitting of low-res blue spectra (R$\sim$2000) with synthetic spectra of varying abundance (Boone et al. 2006). Internal 1-σ level uncertainties are believed to be $\sim$ 0.10 dex.

2.3. *Lithium Abundances*

The basic physical parameters for each star were utilized to linearly interpolate model atmospheres from the Kurucz ATLAS9 atmosphere grids. These model atmospheres were then used in conjunction with the comprehensive line list from King et al. (1997) to compute synthetic spectra with various Li abundances using the most recent version of the spectral synthesis tool MOOG (Sneden 1973). The chosen models introduce an uncertainty into the lithium abundances of 0.03 dex, determined by comparing synthetic lithium synthesis for a standard Kurucz solar model and one developed using our interpolated model atmospheres. The synthetic spectra were smoothed appropriately by convolving them with Gaussians having FWHM values measured from clean, weak lines (continuum depths $\leq$0.2) in multiple orders for each star using the spectrum analysis tool SPECTRE (Fitzpatrick & Sneden 1987).

We positively identified lithium in 7 of the 13 stars in the sample. We derive upper limits for the other 6 stars. We attempted to determine equivalent width errors based on the photon noise methods of Cayrel (1988), but found 1-σ errors $\leq$1.0 mÅ, which are significantly smaller than the uncertainty in continuum placement. In lieu of a more rigorous treatment, we choose to adopt a conservative equivalent width error estimate of 4 mÅ. By

performing additional lithium syntheses for each of the stars, we translate this equivalent width uncertainty to an upper limit in lithium abundance for each star. Sample syntheses are presented in Figure 1.

Appropriate uncertainties in the lithium fits were derived by estimating the goodness of fit by means of an F-test of relative χ^2 values and by adding in quadrature an approximate uncertainty of logN(Li)$\pm$0.08 for a temperature uncertainty of $\pm$100. The typical error in the lithium abundances are found to be $\sim$0.06 dex. The synthetic lithium abundances are given, with their respective errors, in Table 2. We also plot our lithium abundances versus effective temperatures for both the stars in our sample and stars in the $\sim$100 Myr Pleiades cluster (Figure 3). The Pleiades data are taken from Soderblom et al. (1993), Jones et al. (1996), and King et al. (2000) .

2.4.   Radial Velocities and UVW Kinematics

Radial velocities were derived via cross-correlation analysis using the IRAF packages FX-COR and RVCOR. We used HIP 90485 as our template spectrum and adopted its CORAVEL radial velocity of -17.4 $\pm$ 0.2 kms^{-1} (Nordström et al. 2004). Whenever possible, we compared our radial velocities with precise determinations from the literature. In all cases, our velocities matched within the adopted errors. These radial velocities and errors are shown in Table 3. The quoted errors are the internal uncertainties from fitting the cross-correlation functions. Total radial velocity uncertainties are larger than the cross-correlation fitting uncertainties inasmuch as $\sim$2 kms^{-1} intranight telluric line shifts are observed.

The cross-correlation peaks used in the radial velocity determinations confirmed that both HIP 54529 and HIP 63322 were members of binary systems. This was readily apparent in the double lined spectrum of HIP 54529, but HIP 63322 showed no indication of double lines. The asymmetry of the radial velocity cross-correlation peaks showed this star's binary nature.

Space motions were derived with an updated version of the code used by Johnson & Soderblom (1987) which accounts for covariances. The required inputs, UVW Kinematics, and uncertainties are given in Table 3.

3. RESULTS AND DISCUSSION

3.1. *Post T Tauri Status Evaluation*

We utilize three different indicators to assess the evolutionary classification of our stars (summarized in Table 5). First is the lithium abundance. We plot in Figure 3 our derived lithium abundances against effective temperatures for each star, and lithium abundances in the Pleiades cluster from King et al. (2000); they utilized temperatures and lithium abundances derived from both B-V and V-I color indices which we averaged to find a single temperature and abundance. Those stars with abundances that place them in the observed lithium abundance trend of the Pleiades are qualitatively classified as likely being young. Those stars which have measureable Li, yet lie below the Li trend of the Pleiades have inconclusive results about youth. Finally, those stars which have no measurable lithium (i.e. upper limits) are stipulated to most likely be older stars, and unlikely post T Tauri candidates.

Chromospheric activity also provides a useful estimate of youth. In Figure 4 we plot the chromospheric activity index $logR'_{HK}$ (from the recent chromospheric Ca II H and K survey of nearby (d $\leq$ 60 pc) late F through early K dwarfs of D. Soderblom) versus color index for each of our stars. We separate this plot into four distinct activity levels, following the works of Henry et al. (1996) and Gray et al. (2003). We classify those stars with $logR'_{HK}$ greater than -4.75 as either active or very active, and therefore, young targets. It can be noted in Fig. 4 that many of the stars have activities resting in the inactive zone, yet are still near to the active part. While it is unlikely that activity variations are entirely due to stellar variability we note that activity can be at least partially diminished by various effects (i.e. Maunder Minimum phases). With this in mind, we label these stars with inconclusive ages based on chromospheric emission. Those stars which rest in the very inactive category are classified as unlikely to be young.

Third, we utilize UVW kinematics to discern additional qualitative age information. We plotted our stars in the U-V plane (Fig. 5) for comparison with locations of both 'early-type' groups (young main sequence stars of spectral types B-F) and 'late-type' groups (a mixture of young and old main sequence stars of spectral type F-M) in figures 8 and 10 of Skuljan et al. (1999). When a star clearly resides outside of any structures depicted as being young they are classified as likely being older stars. In doing so, we identified several potential members (HIP 47007, HIP 47202, HIP 104903) of the alleged Wolf 630 moving group of Eggen (1969). Youth is difficult to confirm from kinematics alone, therefore the U-V plane was primarily used to exclude older objects. While no conclusive results can be determined, the UVW kinematics did provide a useful criteria for confirming stars with lower lithium abundance

and lower activity as being old.

We considered the above 3 criteria in interpreting evolutionary status from the H-R diagram. In order to describe a star as being young we require 1) a measurable lithium abundance at least as high as that observed in the Pleiades 2) classification of chromospheric activity as either very active or active and 3) non-membership in "old" structures in the U-V plane. The stars which satisfied these criteria are deemed to likely be young stars and mass and age estimates are determined from pre-main sequence mass tracks and isochrones of D'Antona & Mazzitelli (1997). The lithium, chromospheric emission, and kinematic criteria suggest that some of our objects (HIP 90004, HIP 90485, HIP 104903, HIP 47007, HIP 47202) are post ZAMS. Ages are not derived for these stars, as we have successfully eliminated them from consideration as post T Tauri candidates.

3.2. *Ages*

Ages were derived in the standard manner from the most recent pre-main sequence isochrones of D'Antona & Mazzitelli (1997). Examining the positions of our stars in the H-R diagram we found them to lie above or very near the main sequence. We take an age of 100 Myr as indicative of membership on the zero-age main sequence, which is confirmed by the coincidence of single Pleiades stars from King et al. (2000) with the 100 Myr isochrone.

Figure 6 contains our PTT candidates, the D'antona isochrones for ages of 10, 20, 30, 50 and 100 Myrs, and the mass tracks from D'Antona & Mazzitelli (1997). Uncertainties in age are internal and are derived entirely from H-R diagram position and do not account for systematic effects in the models. Errors from convection treatments and opacity effects are not considered. We also examined derived ages and masses using track from both Baraffe et al. (1998) and Siess et al. (2000) to determine the consistency of our derived ages. The isochrones all give similar ages within the error bars. The mass tracks from Baraffe et al. (1998) are shifted to lower T_{eff} resulting in higher mass estimates, particularly for the lower mass stars. Mass differences appear to be as great as 0.07 M$\odot$ around 0.80 M$\odot$ and diminish to 0.02 M$\odot$ at a mass of 1.05 M$\odot$. The mass estimates from Siess et al. (2000) tracks agree well with those from D'Antona & Mazzitelli (1997).

3.3. *Individual Stars*

We present results for each of the stars in the sample. Those stars which we classify as post T Tauri are given in bold.

HIP 47007/HD 82943.—The HIP 47007 lithium abundance (logN(Li)=2.33) lies a factor of 5-6 below the Pleiades distribution; the abundance is more consistent with the older ($\sim$ 600 Myr) Hyades distribution (Fig. 5 of Balachandran (1995)). The chromospheric emission clearly makes this star inactive (logR$'_{HK}$=-4.84). The implied older age is confirmed by the *U-V* plane, where this star appears to reside in the Wolf 630 moving group region. Its position in the H-R diagram indicates the star is post ZAMS.

HIP 47202/HD 83443.—This star's Li upper limit (logN(Li)<0.40) and low chromospheric emission (logR$'_{HK}$=-4.85) suggest an old designation. Indeed, its location in the *U-V* plane is in the middle of the Wolf 630 moving group. While the super-solar metallicity (Fe/H = 0.20) may have led to greater standard PMS convective lithium depletion, its evolutionary status as a post ZAMS is heavily implied by its low activity, its kinematic plane position and its HR diagram position.

HIP 54529A/BD +83 319A.—The Pleiades-like abundance of lithium in the primary was found to be logN(Li)=1.21; we believe the effects of continuum dilution on this abundance to be very small (a few percent). This is the only star for which a chromospheric emission index was not available. However, we compare the level of Hα emission with that of other stars in our sample in Figure 7. The high level of Hα emission is comparable to the amount of emission seen in the most active star in the sample, leading us to label this object as very active. We derive an age of $25\pm^{55}_{15}$ Myr and a mass of 0.83 ± 0.09 M$\odot$ from H-R diagram position. Given the young age and no negative indication of youth from the kinematics, we designate this star as post T Tauri.

HIP 59152/BD +19 2531.—This star has no measurable lithium. We set an upper limit of logN(Li)<0.10. The moderate level of chromospheric emission (logR$'_{HK}$=-4.52) places it along the boundary between the active and inactive class; therefore, age results from this criterion are inconclusive. Position in the *U-V* kinematic plane is inconclusive. Its location places it inside of the Sirius branch (Skuljan et al. 1999). For this star, the lack of evidence of youth from activity and kinematics and the presence of very little lithium make this star unlikely to be a good post T Tauri candidate.

HIP 62758/HD111813.—This star has a near-Pleiades lithium abundance of logN(Li)=1.67; its chromospheric emission (logR$'_{HK}$=-4.32) places it in the active category. These two findings suggest possible youth not inconsistent with its location in the *U-V* plane. Using the H-R diagram we derive an age of $47\pm^{30}_{10}$ Myr and a mass of 0.78 ± 0.02 M$\odot$. Recognizing that, within the errors, this star is nearly on the ZAMS we classify it as a PTT or ZAMS star.

HIP 63322/BD+39 2587.—We find an appreciable abundance of lithium in this

star (logN(Li)=1.60). Its chromospheric emission ties for the highest of any of the stars in the sample (logR$'_{HK}$-4.12). Location near the Pleiades branch (Saffe et al. 2005) in the kinematic plane is consistent with youth. The age (45 $\pm^{15}_{13}$Myr) derived from the location in the H-R diagram, coupled with the significant Li and chromospheric emission, leads us to label this star as post T Tauri. We find a rough estimate of the mass, assuming it was a single star, of 0.77 $\pm$ 0.03 M$\odot$. We also note again that the line profiles and the cross-correlation peaks exhibit a notable asymmetry, indicative of this star being a spectroscopic binary.

HIP 74045/HD135363.—HIP 74045 is the only broad-lined star of the sample, suggesting a moderate projected rotation ($\sim$15 km/s) consistent with youth. The substantial lithium abundance (logN(Li)=1.96) lying in the midst of the Pleiades' distribution is also suggestive of youth. The chromospheric emission (logR$'_{HK}$=-4.17) places this star in the very active category. Finally, this object does not reside in any older U-V kinematic plane structures. The location in the H-R diagram confirms youth and a PTT classification with an age of 36 $\pm^{14}_{6}$ Myr and a mass of 0.78 $\pm$ 0.01 M$\odot$.

HIP 87330/HD162020.—Our upper limit to the lithium abundance of HIP 87330 (logN(Li)<-0.30) lies a factor of 10 below the Pleiades trend, suggesting a post ZAMS age. However, the chromospheric emission index (logR$'_{HK}$=-4.12) taken from Saffe et al. (2005), ties for the highest in the sample. The kinematics of the star yield inconclusive results. With the lack of correlation between the low lithium abundance and high chromospheric emission we hesitate to make any definitive conclusions on the nature of this star.

HIP 90004/HD168746.—This star has an upper limit to its lithium abundance of logN(Li)<0.90. The chromospheric emission index (logR$'_{HK}$=-5.11) is the lowest in the sample. While its position in the U-V plane is inconclusive, the low lithium upper limit, the extremely low emission index and H-R diagram position imply this star is post ZAMS.

HIP 90485/HD169830.—We set an upper limit on this star of logN(Li)<1.5. The chromospheric emission is also extremely low (logR$'_{HK}$=-4.93). Although the position in the U-V kinematic plane is inconclusive, the low lithium upper limit coupled with the low emission index clearly indicate that this star's location above the main sequence on the H-R diagram is due to its status as a post ZAMS star.

HIP 104864/HD202116.—This star shows a high lithium abundance of logN(Li)=2.50, which lies just below the Pleiades trend. The emission index of logR$'_{HK}$=-4.37 places this star in the active category. The U-V kinematics do not place this star within any old moving group structures. While these three indications imply youth for the star, the position in the H-R diagram shows that, within the errors, this star could reside on the main sequence. We derive an age of 29 $\pm^{21}_{5}Myr$ and a mass of 1.03 $\pm$ 0.02 M$\odot$. While this

age makes the star a post T Tauri candidate, its location in the H-R diagram shows that a ZAMS classification remains plausible.

HIP 104903/HD 202206.—This star exhibits a low Li abundance (logN(Li)=1.10), placing it well below the Pleiades distribution. The chromospheric emission of logR$'_{HK}$=-4.81 places it in the inactive category, implying a slightly older star. Indeed, the position in the *U-V* plane leads to classification of this star as a potential member of the alleged 5 Gyr Wolf 630 moving group of Eggen (1969). Its position in the H-R diagram indicates the star is post ZAMS.

HIP 114007/BD -07 5930.—The star has an upper limit lithium abundance of logN(Li) < 0.30 and an extremely low chromospheric emission index (logR$'_{HK}$-4.74). The object's position in the kinematic plane is inconclusive. The low lithium upper limit and the low chromospheric emission, coupled with the position on the H-R diagram, lead to this star's classification as ZAMS or older.

3.4. *Irregular Variability*

We used the *HIPPARCOS* Epoch Photometry Annex to examine photometric variability in the 5 PTT candidates. This tool provided all the photometric measurements from the *HIPPARCOS* mission for the stars in our sample. We used these to construct histograms of the reduced chi-squared (χ^2_ν) and the real dispersion (σ_{real}) of the V magnitudes about their average. We calculate the difference in the observed and expected variances as the real variance.

For comparison, we performed the same analysis on a sample of the 25 best solar analog candidates from tables 5,6 and 7 of Cayrel de Strobel (1996). These analogs provide a solid baseline of inactive stars that are presumably not subject to irregular variability. Additionally, we performed this analysis for 15 classical T-Tauri stars from the emission line star catalog of Herbig and Bell (Herbig & Bell 1995) with available *HIPPARCOS* data. The solar analogs and T Tauri stars provide the context of a large range of anticipated variability to fit our post T Tauri stars into. We also include 41 post T Tauri aged stars taken from the literature (Mamajek et al. 2002) to increase the PTT sample size and compare with our candidates. The χ^2_ν and σ_{real} can be seen in Figure 8.

The T Tauri stars clearly show random variability. The majority have both χ^2_ν values and real dispersions nearly an order of magnitude greater than the PTTs and solar analogs.

The majority of the solar analogs cluster around $\chi^2_\nu \sim 1$. This shows that the analogs

tend to have magnitudes close to their average, i.e. that they are much less variable. Furthermore, the dispersion histogram also shows that the analogs stay clustered close to their average magnitudes with the typical dispersion $\sigma_{real} \leq 0.01$ mag.

The χ_ν^2 and σ_{real} of our post T Tauri candidates fit nicely in the range exhibited in the literature sample, between χ_ν^2 values of 1 and 4, lending further credence to their selection as candidates. Also, notice the dispersions of the post T Tauri magnitudes are both lower and less widespread than those of the TTs. They are not as variable as their precursors. Examining the overall picture, notice that both the χ_ν^2 and σ_{real} are intermediate between the values exhibited by T Tauri stars and solar analogs as expected.

We performed a Kolmogorov-Smirnov (K-S) test of the distributions to quantitatively explore the differences between the histogram distributions. The K-S test comparing the distribution of both the real dispersions (σ_{real} and χ_ν^2) values for T-Tauri stars and our post T Tauri stars revealed that the two samples were not drawn from the same distribution. Comparing the PTT sample from the literature with the PTTs of this paper, we found them to be drawn from a similar distribution. Finally, the K-S test for our PTTs and solar analogs revealed that the two cumulative samples were drawn from different distributions. The K-S tests then solidify our PTT classications to the extent that they confirm that PTT stars have an intermediate degree of irregular variability between T Tauri stars and solar analogs, as anticipated.

3.5.   *Infrared Excess*

For the sake of completeness we conducted a search for any irregularities in the PTT SED's, traced by Johnson BVI_C photometry, 2MASS JHK_s photometry and IRAS and SPITZER photometry when available. Considering the proximity of these stars (within 60 parsecs of the Sun), we did not anticipate that they would be affected by insterstellar reddening. However, to determine the extent to which reddening may have an affect we created a reddening sensitive Johnson-band color-color diagram of (J-K) versus (V-K), following Carney (1983). The stars in our sample were clearly seen to lie along a trend of unreddened, single stars of the Hyades cluster. This implies that they are not susceptible to interstellar reddening.

After establishing that reddening corrections were unnecessary, we converted the relevant magnitudes to flux densities (in Jansky) for comparison with Kurucz model photospheric fluxes (Castelli & Kurucz 2003), normalized at I_C. We chose to normalize to the I_C magnitudes. Two of the 5 PTTs we identified showed significant near-infrared excesses (HIP 63322,

HIP 74045). However, we reserve judgement on the authenticity of the observed excess in these two cases because using a J-band normalization yields no sign of excess in any of the stars (Fig.(9)). Indeed, in contrast to the results of Cieza et al. (2005) on JHK excesses in CTTs, we find that a J-band normalization slightly improves the fit to the SED at other wavelengths.

In order to examine the likelihood that a PTTs would exhibit a near-IR excess, we performed the same analysis on a literature sample of 16 post T Tauri stars (Mamajek et al. 2002), who utilize spectral-type based Teff values. The sample analyzed showed that excess was present in approximately 50 percent of the stars analyzed. To further examine our methodology, we analyzed a sample of presumably unremarkable solar analogs to confirm that no spurious effects were present. None of the solar analogs analyzed exhibited any form of infrared excess. In Figures 10 and 11 we present SEDs for our stars as well as a sample of solar analogs and literature post T Tauri stars.

The observed SEDs of many objects in the literature sample of post T Tauri stars seemed to match the morphology of our post T Tauri candidates of lower Teff thus we calculated photometric temperatures for each of the literature stars and performed a Kurucz model flux fit using these photometric temperatures. The model fluxes characterized by photometric temperatures fit the observed SEDs better than those characterized by the literature-based effective temperature values (Fig. 12) which are 250-1000 K higher. This indicates that photometric temperatures may be more reliable than those determined from spectral type calibrations for the cooler PMS stars or the log(g)-based decrements used by Mamajek et al. (2002) are too small.

3.6. Hα Equivalent Widths

Hα emission provides a strong indication of youth in a star. However, if we consider Hα emission relative to our other indicators of youth, it has the smallest decay time. So, while high levels of emission imply youth, low levels of emission (or high levels of absorption) do not necessarily discredit youth. For completeness, measurements of the equivalent widths of the Hα feature for each of the stars in the sample are presented in Table 4 since these line strengths are often used in classifying CTTs.

We note that the binary star HIP 63322 exhibits a P-Cygni profile in the Hα region, a feature that is common in many classical T Tauri stars; however, the EW is too low to suggest such a classification. The blueshifted absorption feature can be attributed to a strong stellar wind, however, a small redshifted absorption feature also appears to be present. Data

with the Hα line centered away from the edge of the CCD are needed to examine this feature and determine if it is "real". If it represents an actual absorption, this could be indicative of infall onto one of the members of the system, making this a particularly interesting example of a post T Tauri system.

4. SUMMARY

We have utilized an age-oriented analysis to identify 5 isolated post T Tauri candidates (HIP 54529, HIP 62758, HIP 63322, HIP 74045, HIP 104864) and analyzed their irregular variability and SEDs. The irregular variability of our candidates, and PTTs in general, appear to be intermediate in nature to T Tauri and solar analog variability. Two of the 5 candidates (HIP 63322 and HIP 74045) exhibit near-IR excesses when normalized to the I_C, although this same excess is non-existent with a J-band normalization. Subsequent study must be undertaken to determine the nature and validity of these excesses. In our SED analysis, we also find that model fluxes based on photometric temperatures appear to match observed SEDs better than model fluxes using temperatures based on spectral standards. Also of note is the binarity of 2 of our post T Tauri stars: HIP 54529 and HIP 63322 are found to be spectroscopic binaries.

Our combination of H-R diagram positions and various qualitative indicators of youth (including lithium abundances, chromospheric emission and kinematics) appears to be a robust means to select samples of nearby, young, isolated post T Tauri stars that would otherwise masquerade as normal field stars. The method that we have developed will be applied to larger samples of stars to further enhance the population of known post T Tauri stars.

REFERENCES

Allende Prieto, C., Barklem, P. S., Lambert, D. L., & Cunha, K. 2004, A&A, 420, 183

Balachandran, S. 1995, ApJ, 446, 203

Baraffe, I., Chabrier, G., Allard, F., & Hauschildt, P. H. 1998, A&A, 337, 403

Boesgaard, A. M., & Tripicco, M. J. 1986, ApJ, 303, 724

Boone, R. H., King, J. R., & Soderblom, D. R. 2006, New Astronomy Review, 50, 526

Butler, R. P., et al. 2006, ApJ, 646, 505

Carney, B. W. 1983, AJ, 88, 623

Castelli, F., & Kurucz, R. L. 2003, Modelling of Stellar Atmospheres, 210, 20P

Cayrel, R. 1988, IAU Symp. 132: The Impact of Very High S/N Spectroscopy on Stellar Physics, 132, 345

Cayrel de Strobel, G. 1996, A&A Rev., 7, 243

Cieza, L. A., Kessler-Silacci, J. E., Jaffe, D. T., Harvey, P. M., & Evans, N. J., II 2005, ApJ, 635, 422

Cutri, R. M., et al. 2003, The IRSA 2MASS All-Sky Point Source Catalog, NASA/IPAC Infrared Science Archive. http://irsa.ipac.caltech.edu/applications/Gator/,

D'Antona, F., & Mazzitelli, I. 1997, Memorie della Societa Astronomica Italiana, 68, 807

Eggen, O. J. 1969, PASP, 81, 553

Fitzpatrick, M. J., & Sneden, C. 1987, BAAS, 19, 1129

Gray, R. O., Corbally, C. J., Garrison, R. F., McFadden, M. T., & Robinson, P. E. 2003, AJ, 126, 2048

Henry, T. J., Soderblom, D. R., Donahue, R. A., & Baliunas, S. L. 1996, AJ, 111, 439

Herbig, G. H. 1978, Problems of Physics and Evolution of the Universe, 171

Herbig, G. H., & Bell, K. R. 1995, VizieR Online Data Catalog, 5073, 0

Israelian, G., Santos, N. C., Mayor, M., & Rebolo, R. 2004, A&A, 414, 601

Jensen, E. L. N. 2001, ASP Conf. Ser. 244: Young Stars Near Earth: Progress and Prospects, 244, 3

Johnson, D. R. H., & Soderblom, D. R. 1987, AJ, 93, 864

Jones, B. F., Shetrone, M., Fischer, D., & Soderblom, D. R. 1996, AJ, 112, 186

King, J. R., Deliyannis, C. P., Hiltgen, D. D., Stephens, A., Cunha, K., & Boesgaard, A. M. 1997, AJ, 113, 1871

King, J. R., Krishnamurthi, A., & Pinsonneault, M. H. 2000, AJ, 119, 859

Mamajek, E. E., Meyer, M. R., & Liebert, J. 2002, AJ, 124, 1670

Nordström, B., et al. 2004, A&A, 418, 989

Perryman, M. A. C., & ESA 1997, The Hipparcos and Tycho catalogues. Astrometric and photometric star catalogues derived from the ESA *HIPPARCOS* Space Astrometry Mission, Publisher: Noordwijk, Netherlands: ESA Publications Division, 1997, Series: ESA SP Series vol no: 1200, ISBN: 9290923997 (set),

Petrov, P. P. 2003, Astrophysics, 46, 506

Ramírez, I., & Meléndez, J. 2005, ApJ, 626, 465

Saffe, C., Gómez, M., & Chavero, C. 2005, A&A, 443, 609

Santos, N. C., Israelian, G., & Mayor, M. 2004, A&A, 415, 1153

Schuler, S. C., King, J. R., Terndrup, D. M., Pinsonneault, M. H., Murray, N., & Hobbs, L. M. 2006, ApJ, 636, 432

Siess, L., Dufour, E., & Forestini, M. 2000, A&A, 358, 593

Skuljan, J., Hearnshaw, J. B., & Cottrell, P. L. 1999, MNRAS, 308, 731

Sneden, C. 1973, ApJ, 184, 839

Soderblom, D. R., Jones, B. F., Balachandran, S., Stauffer, J. R., Duncan, D. K., Fedele, S. B., & Hudon, J. D. 1993, AJ, 106, 1059

Soderblom, D. R., et al. 1998, ApJ, 498, 385

Zuckerman, B., & Song, I. 2004, ARA&A, 42, 685

Table 1.   Log of Observations, 2000 May 28-29 UT

HIP	BD/HD	V	B-V	MJD [a] 51692+	Exposure Time (sec)	S/N
47007	HD 82943	6.53	0.625	0.263922	120	464
47202	HD 83443	8.23	0.814	0.267599	300	266
54529A	BD +83 319A	9.93	0.949	0.276696	300	159
59152	BD +19 2531	9.19	0.884	0.282785	300	267
62758	HD 111813	9.09	0.907	0.302474	180	222
63322	BD +39 2587	9.27	0.855	0.291452	180	193
74045	HD 135363	8.72	0.949	0.369162	120	198
87330	HD 162020	9.18	0.968	0.446854	300	247
90004	HD 168746	7.95	0.713	0.452436	180	320
90485	HD 169830	5.91	0.518	0.456642	60	447
104864	HD 202116	8.39	0.614	0.610233	120	210
104903	HD 202206	8.08	0.714	0.613773	300	386
114007	BD -07 5930	9.55	1.069	0.619408	180	165

[a]MJD=JD-2400000.5

Table 2.   Stellar Parameters

HIP	BD/HD	B-V	V-K$_{2mass}$	M$_V$	T$_{eff}$	log(g)	ξ kms^{-1}	logR$\prime_{HK}$	logN(Li)	[M/H]
47007 [a]	HD 82943	0.625	1.425	4.337	5851 $\pm$ 49	4.21 $\pm$ 0.09	1.05	-4.837	2.33 $\pm$ 0.08	0.0
47202 [a]	HD 83443	0.814	1.786	5.036	5313 $\pm$ 50	4.24 $\pm$ 0.16	1.26	-4.850 [b]	$\leq$ 0.40	0.20
54529A [c]	BD +83 319A	0.949	2.628	6.164	4668 $\pm$ 162	4.36 $\pm$ 0.55	0.98	$\cdots$	1.10 $\pm$ 0.06	-0.14
59152	BD +19 2531	0.884	2.162	6.203	4947 $\pm$ 50	4.44 $\pm$ 0.19	1.08	-4.523	$\leq$ 0.10	0.00
62758	HD 111813	0.907	2.096	6.210	4990 $\pm$ 49	4.45 $\pm$ 0.18	1.10	-4.320	1.67 $\pm$ 0.06	-0.10
63322 [d]	BD +39 2587	0.855	2.389	6.365	4786 $\pm$ 49	4.45 $\pm$ 0.22	1.01	-4.116	1.60 $\pm$ 0.03	-0.20
74045	HD 135363	0.949	2.529	6.375	4680 $\pm$ 50	4.41 $\pm$ 0.10	0.98	-4.169	1.96 $\pm$ 0.05	-0.10
87330 [a]	HD 162020	0.968	2.641	6.705	4577 $\pm$ 52	4.47 $\pm$ 0.20	0.94	-4.120 [b]	$\leq$ -0.30	0.00
90004 [a]	HD 168746	0.713	1.697	4.777	5477 $\pm$ 52	4.04 $\pm$ 0.17	1.40	-5.107	$\leq$ 0.90	-0.17
90485 [a]	HD 169830	0.518	1.222	3.109	6207 $\pm$ 54	3.95 $\pm$ 0.12	1.81	-4.925	$\leq$ 1.50	0.00
104864	HD 202116	0.614	1.535	4.909	5735 $\pm$ 53	4.37 $\pm$ 0.17	1.39	-4.368	2.50 $\pm$ 0.04	-0.05
104903 [a]	HD 202206	0.714	1.595	4.750	5581 $\pm$ 51	4.18 $\pm$ 0.18	1.39	-4.808	1.10 $\pm$ 0.11	0.13
114007	BD -07 5930	1.069	2.288	6.486	4799 $\pm$ 54	4.43 $\pm$ 0.23	1.03	-4.735	$\leq$ 0.30	-0.05

[a]These stars are all known hosts of extra-solar planets. They also have spectroscopic temperatures available in Santos et al. (2004) and Israelian et al. (2004).

[b]Chromospheric activity indices for these stars were taken from Saffe et al. (2005). All others were taken from the recent chromospheric Ca II H and K survey of nearby (d≤60 pc) late F and early K dwarfs of D. Soderblom.

[c]This star is a double lined spectroscopic binary (SB2). We label it with an 'A', as our analysis is for the primary component. The error on the temperature was determined by taking the RMS deviation of the equivalent width fit of Fig. 2.

[d]This star is a spectroscopic binary (SB1) as revealed by asymmetry in cross-correlation peaks.

Table 3.   Kinematic Infomation

HIP	π	PM RA	PM DEC	Radial Velocity	U	V	W
	mas	mas/yr	mas/yr	kms^{-1}	kms^{-1}	kms^{-1}	kms^{-1}
47007	36.42 ± 0.84	2.38 ± 0.89	-174.05 ± 0.53	8.53 ± 0.44	10.05 ± 0.36	-20.38 ± 0.47	-8.53 ± 0.37
47202	22.97 ± 0.90	22.35 ± 0.72	-120.76 ± 0.69	29.34 ± 0.63	19.94 ± 0.80	-31.26 ± 0.63	-11.82 ± 0.62
54529A	17.65 ± 2.66	-69.59 ± 2.80	-34.35 ± 2.34	-2.04 ± 10.00 [a]	-15.96 ± 5.62	-13.47 ± 6.98	-1.32 ± 5.52
59152	25.27 ± 1.40	120.06 ± 1.54	-73.58 ± 0.72	-5.11 ± 0.55	26.69 ± 1.48	-0.47 ± 0.23	-3.03 ± 0.55
62758	26.54 ± 1.45	-142.59 ± 1.24	-37.49 ± 1.19	-4.06 ± 0.59	-17.79 ± 0.99	-19.38 ± 1.09	-4.04 ± 0.59
63322	26.24 ± 1.75	-126.76 ± 1.33	-42.02 ± 1.22	-12.31 ± 0.85 [b]	-13.84 ± 1.02	-19.38 ± 1.29	-9.97 ± 0.85
74045	33.97 ± 0.69	-131.87 ± 0.62	169.32 ± 0.79	-7.52 ± 1.77	-26.21 ± 0.80	-13.05 ± 1.29	-9.68 ± 1.10
87330	31.99 ± 1.48	20.99 ± 2.35	-25.20 ± 1.27	-27.52 ± 0.59	-27.60 ± 0.58	2.55 ± 0.27	-1.49 ± 0.38
90004	23.19 ± 0.96	-22.13 ± 0.90	-69.23 ± 0.66	-25.51 ± 0.39	-19.15 ± 0.42	-22.04 ± 0.60	-3.11 ± 0.21
90485	27.53 ± 0.91	-0.84 ± 1.23	15.16 ± 0.72	-17.40 ± 0.20	-16.94 ± 0.20	1.18 ± 0.16	3.81 ± 0.20
104864	20.13 ± 1.16	101.39 ± 1.20	-10.22 ± 0.58	-2.87 ± 0.34	-17.77 ± 0.97	-3.31 ± 0.22	-16.01 ± 1.07
104903	21.58 ± 1.14	-38.23 ± 1.36	-119.77 ± 0.49	13.78 ± 0.44	22.11 ± 0.76	-19.53 ± 1.31	-9.36 ± 0.36
114007	24.39 ± 1.75	-172.51 ± 2.01	-201.31 ± 1.46	27.85 ± 0.62	52.83 ± 3.39	-7.24 ± 1.57	-24.44 ± 0.56

[a]The radial velocity is a crude estimate of the systemic velocity of the binary system. It was taken by averaging the velocities of the two cross-correlation peaks in the FXCOR package of IRAF.

[b]This star is an SB1 as indicated by an asymmetric cross-correlation peak in the radial velocity analysis. The velocity for this system should be taken as an estimate.

Table 4.   Hα Equivalent Widths

HIP	Hα EW
	$\mathring{A}$
47007	1.1368
47202	1.0342
54529 [a]	-0.1703
59152	0.9546
62758 [a]	0.8549
63322	0.2521
74045 [a]	-0.2115
87330 [a]	0.6016
90004	1.0409
90485	1.1310
104864	0.9736
104903	1.0233
114007	0.8626

[a]The Hα feature for these stars are plotted in Fig. 7.

Table 5.   Summary of Age-Oriented Analysis Results

HIP	logN(Li)	logR'$_{hk}$	Kinematics	H-R Diagram	Status	Ages [a] Myr	$\delta(Age)$ [b]
47007	yes	no	no	no	Post ZAMS		
47202	?	no	no	no	Post ZAMS		
54529A	yes	yes [b]	?	yes	PTTs	$25\pm^{55}_{15}$	-3.16
59152	no	yes	?	?	ZAMS or Older		
62758	yes	yes	?	?	PTTs or ZAMS	$47\pm^{30}_{10}$	
63322	yes	yes	?	yes	PTTs	$45\pm^{15}_{13}$	-6.93
74045	yes	yes	?	yes	PTTs	$36\pm^{14}_{6}$	-3.38
87330	no	yes	?	yes	$\sim$ZAMS		
90004	no	no	?	no	Post ZAMS		
90485	no	no	?	no	Post ZAMS		
104864	yes	yes	?	?	PTTs or ZAMS	$29\pm^{21}_{5}$	
104903	?	no	no	no	Post ZAMS		
114007	no	no	no	?	ZAMS or Older		

[a]Ages are derived based on the assumption of solar metallicity.

[b]The quantity $\delta(Age)$ gives the difference between ages assuming solar metallicity and ages which account for the sub-solar metallicites. We utilized the online tools of Siess et al. (2000) to interpolate between solar (Z=0.02) and subsolar (Z=0.01) stellar ages to obtain our metallicity sensitive ages. The negative sign indicates that metallicity sensitive ages are younger.

[c]We compare the levels of H-alpha emission of this star with several other stars in the sample in Figure 7. This star is seen to have emission levels similar to those of one of the more chromospherically active stars in the sample, thus we label it as "active".
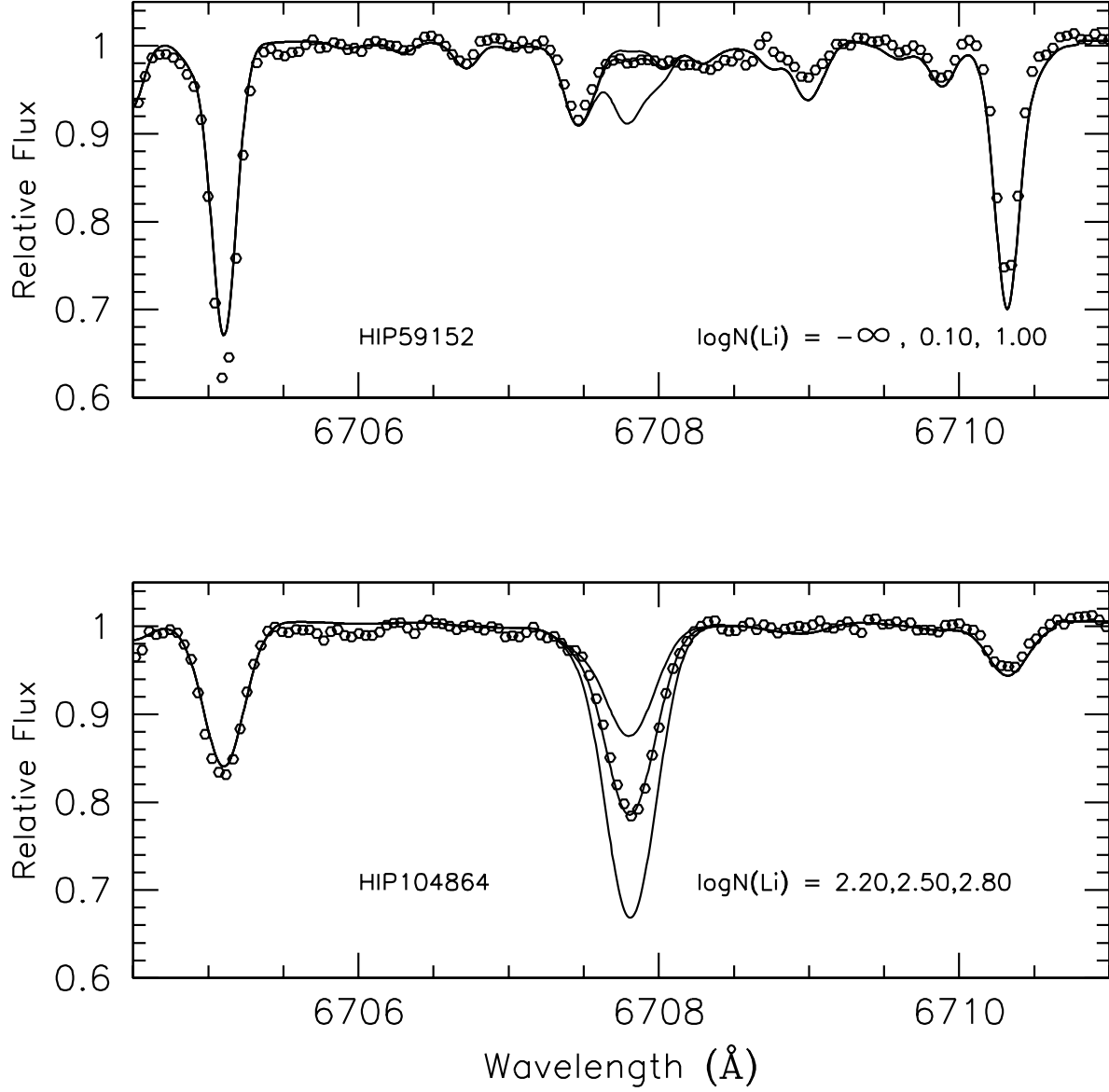
Fig. 1.— Sample Keck HIRES spectra in the Li Iλ6707 region. The observed spectra are plotted as open circles and varying synthesis of lithium abundances are plotted as solid lines. HIP 59152 (top) has an upper limit (logN(Li)≤0.10) on its lithium abundance and HIP 104864 (bottom) is a clear lithium abundance determination (logN(Li)=2.50). The varying lithium synthesis in the positive detection each differ by a factor of 2.
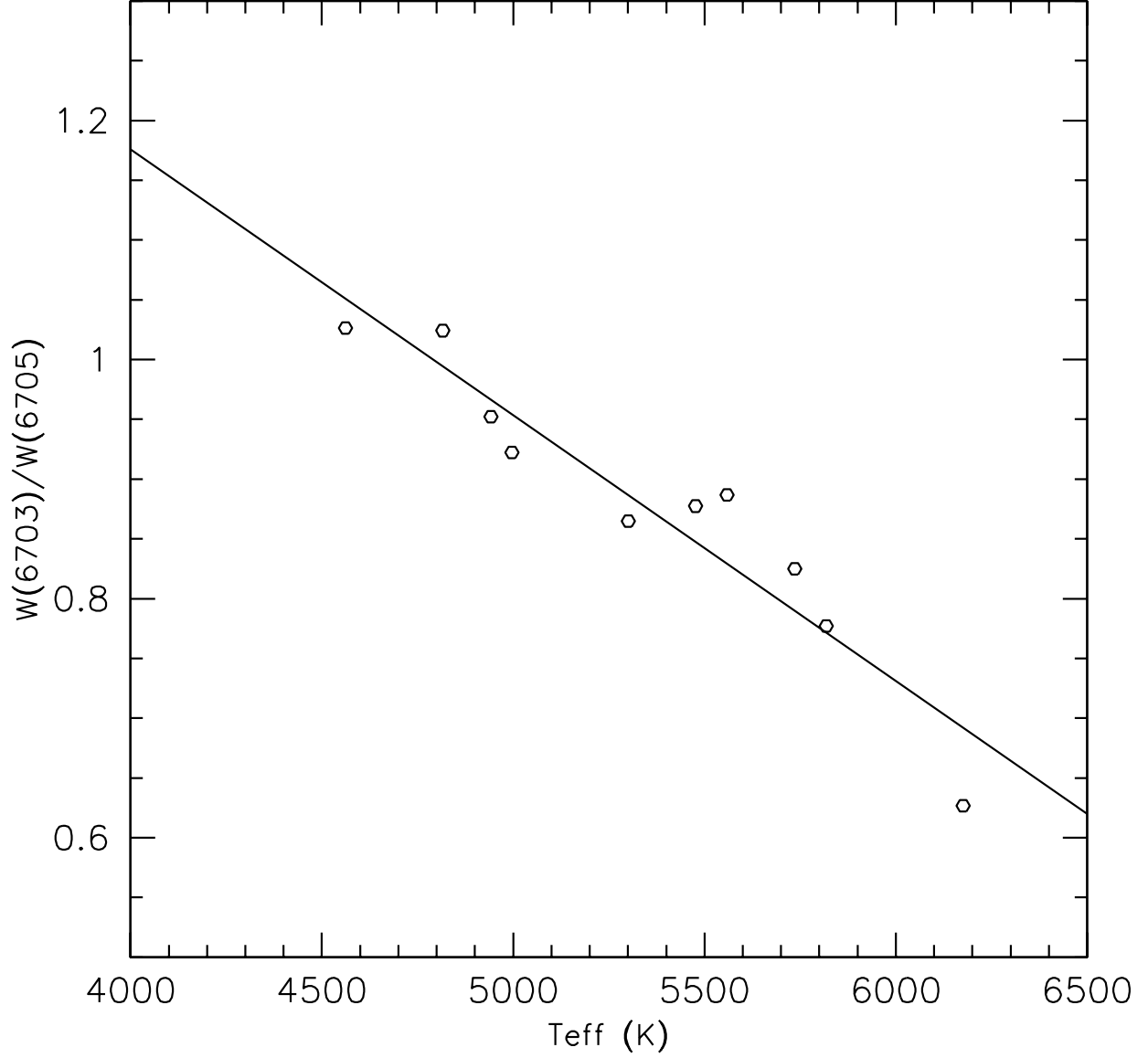
Fig. 2.— Equivalent width ratios of two Fe I lines (λ=6703 and 6705) versus photometric temperatures for the stars in our sample. The line is a least squares fit to the data which was used for estimating temperatures in the primary and secondary components of the double-lined spectroscopic binary HIP 54529. This follows the method outlined by Boesgaard & Tripicco (1986).
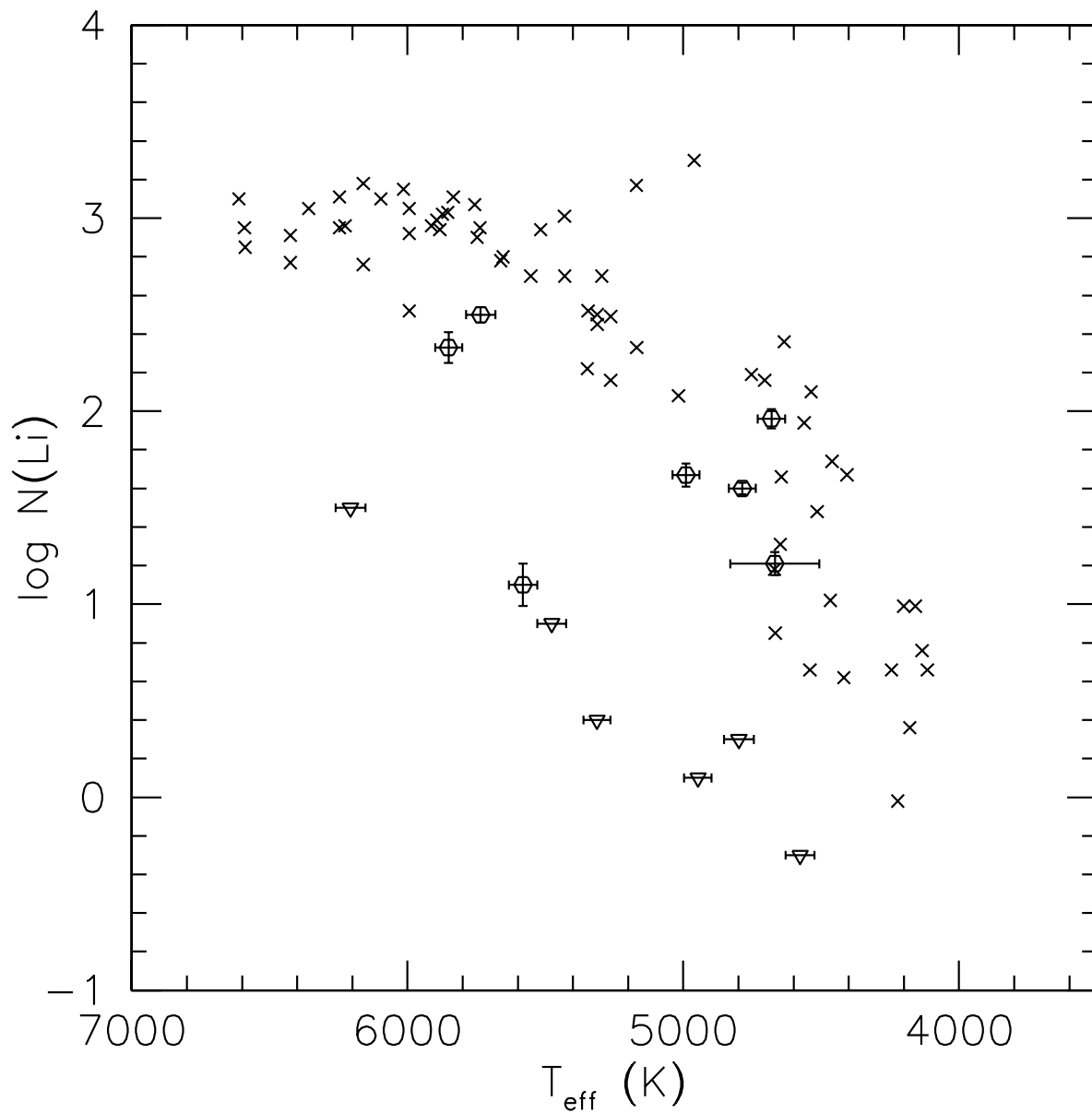
Fig. 3.— Lithium abundances compared to those of the Pleiades star cluster. The Pleiades stars are plotted as x's. Positive identifications of lithium are shown as open hexagons. Upper limits on lithium are plotted as triangles.
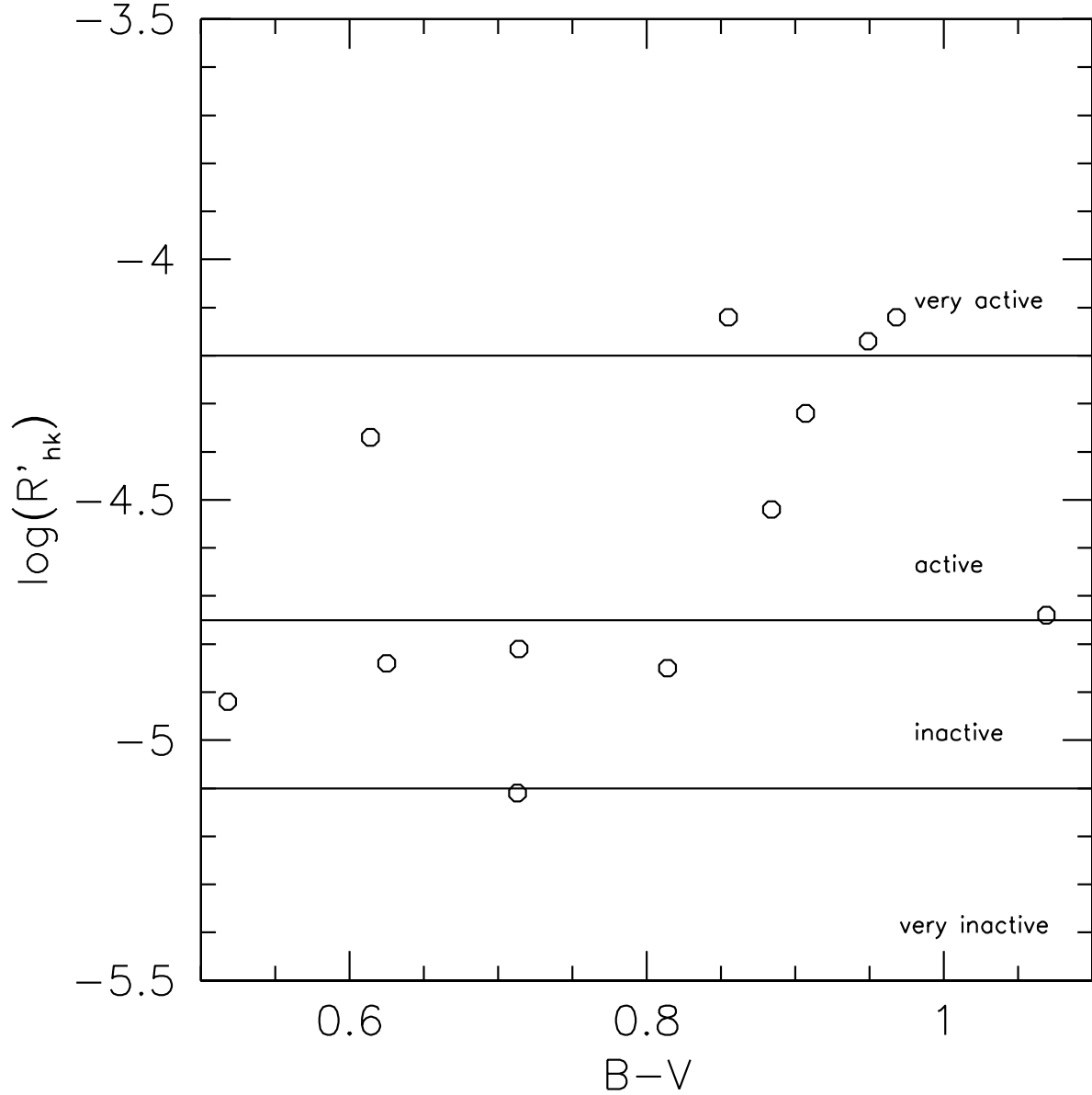
Fig. 4.— Levels of chromospheric emission ($\log R'_{HK}$) given as a function of B-V color index. The activities are separated into four classes of activity following Henry et al. (1996). Stars which are very inactive are likely not the young pre-main sequence stars being sought. Those stars which are either very active or active are likely younger stars making them suitable PTTs candidates. Due to fluctuations in activity cycles (i.e. Maunder minimum-like phases) we cannot rule out inactive stars as old. They could potentially be exhibiting uncharacteristically low levels of chromospheric emission.
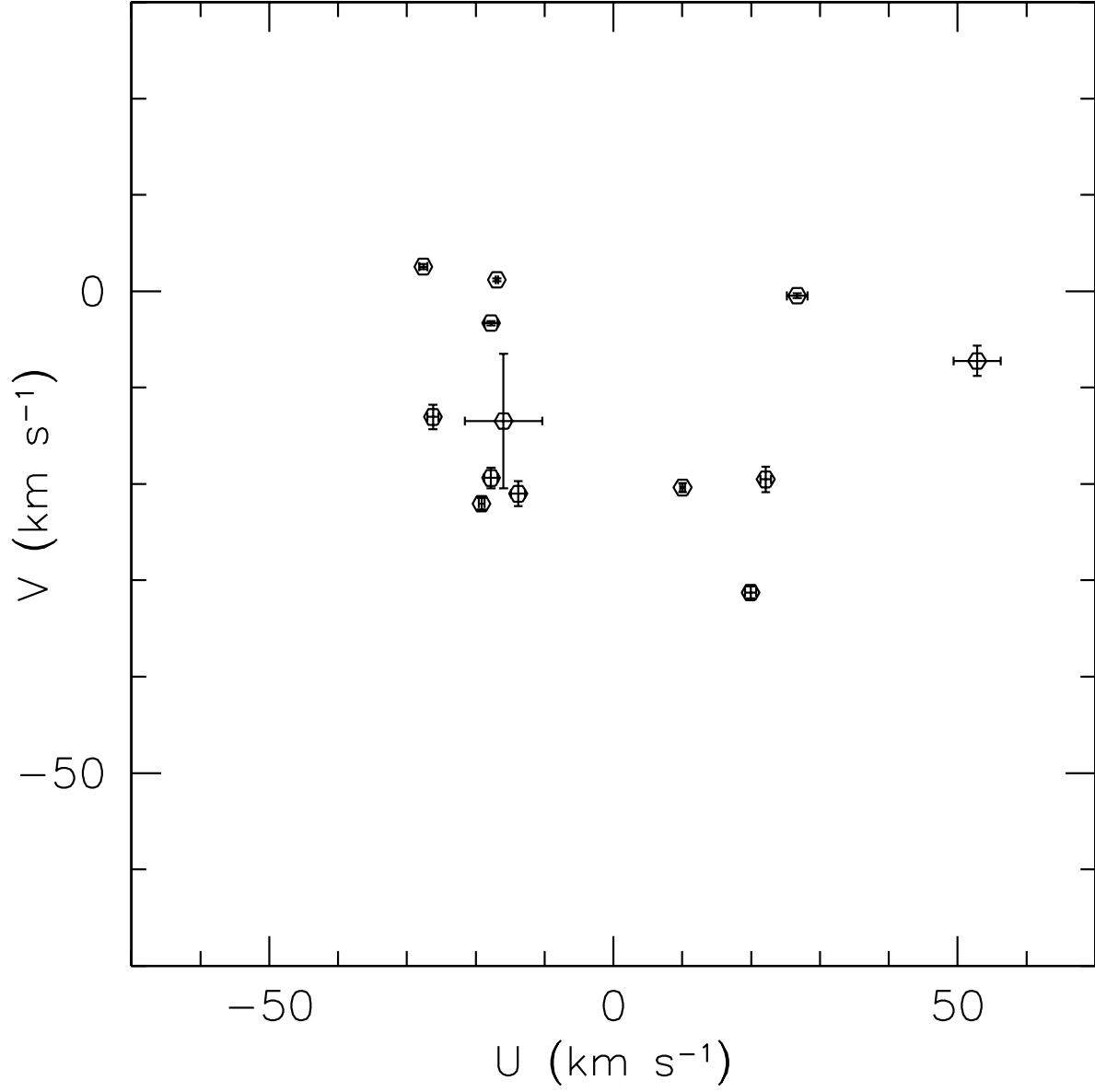
Fig. 5.— Plot of our sample in the *U-V* kinematic plane. We utilized this plot to compare with figures 8 and 10 from Skuljan et al. (1999) to determine membership in moving groups of stars in various evolutionary states.
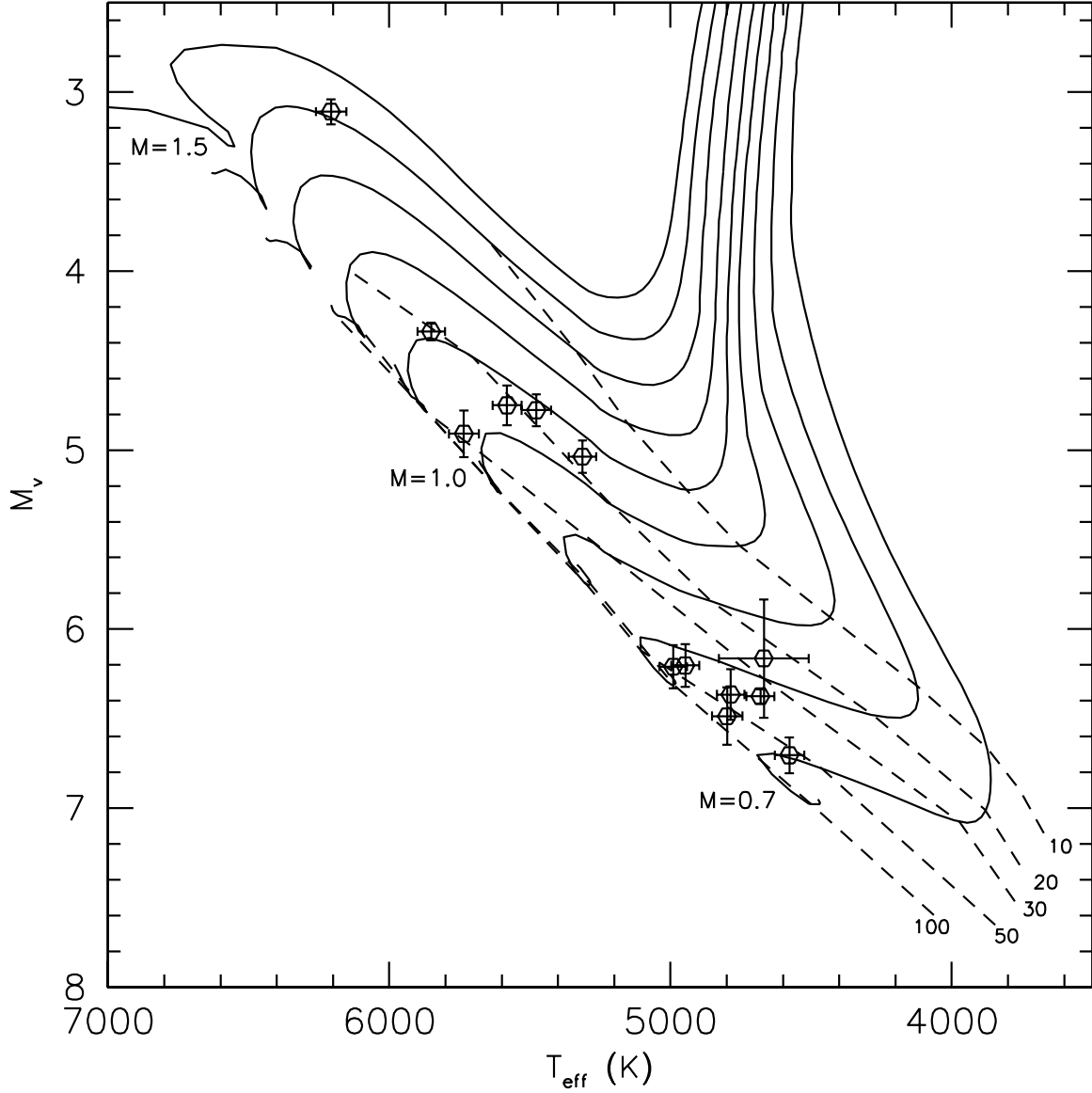
Fig. 6.— H-R Diagram showing positions of the sample with respect to the ZAMS (100 Myr). Mass tracks and isochrones assuming solar metallicity are taken from D'Antona & Mazzitelli (1997). Ages are estimated only for those stars which are confirmed to be post T Tauri stars based on lithium abundances, chromospheric activity, and *UV* kinematics. The isochrone ages are given in Myr. The mass tracks are given in solar masses and increase in increments of 0.1 solar masses.
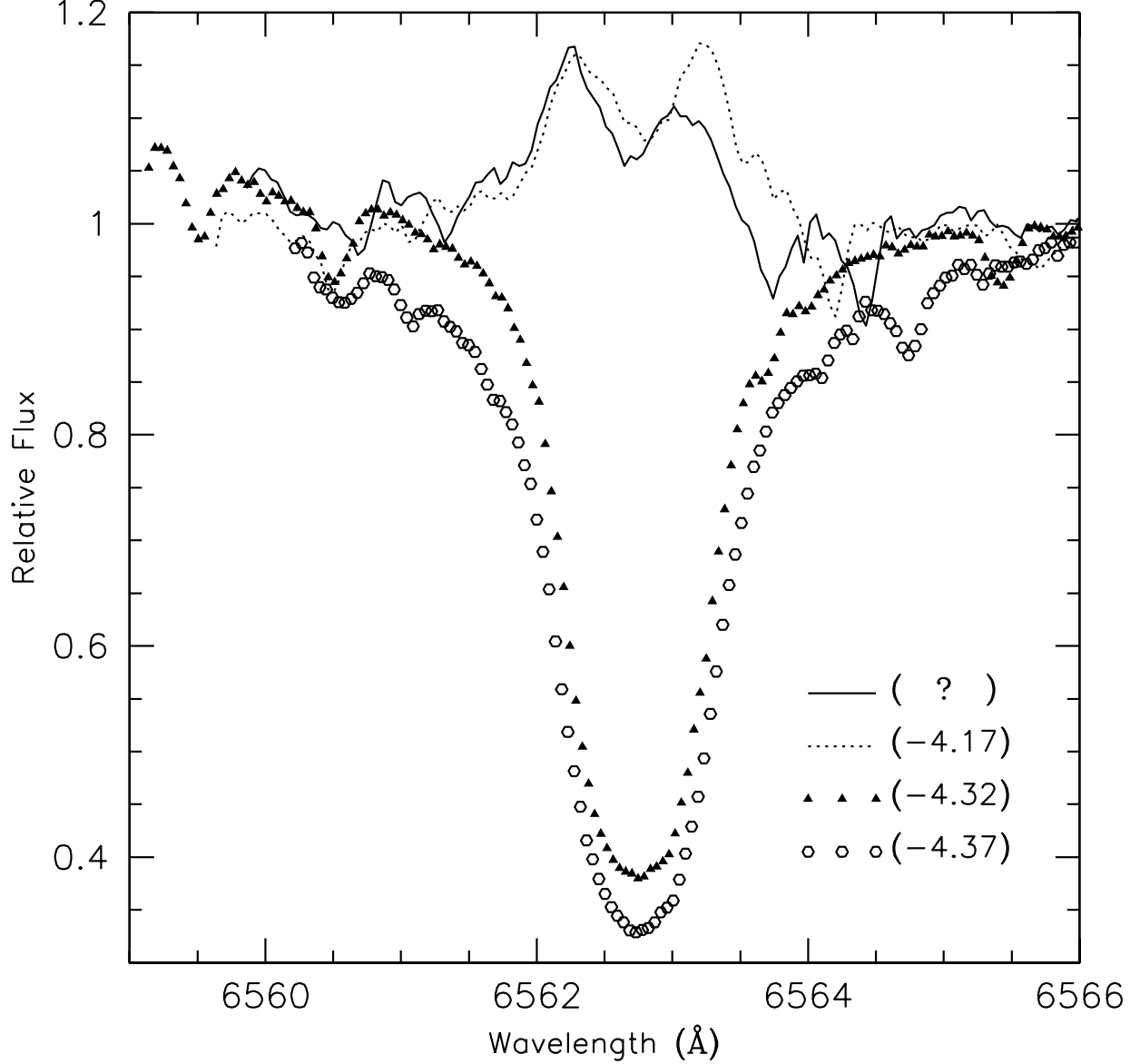
Fig. 7.— Comparison of Hα emission of our double lined binary with other active stars. The legend gives the activity levels of each line type. The solid line is the double lined binary HIP 54529. The dotted line is HIP 74045, one of the candidate PTTs. The open hexagons are HIP 87330, a ZAMS object. The triangles are HIP 62758, a PTT candidate with a modest level of chromospheric activity. The double-lined binary clearly has Hα in emission, implying both youth and high chromospheric emission when compared with HIP 74045, which likewise is in emission and has extremely high activity.
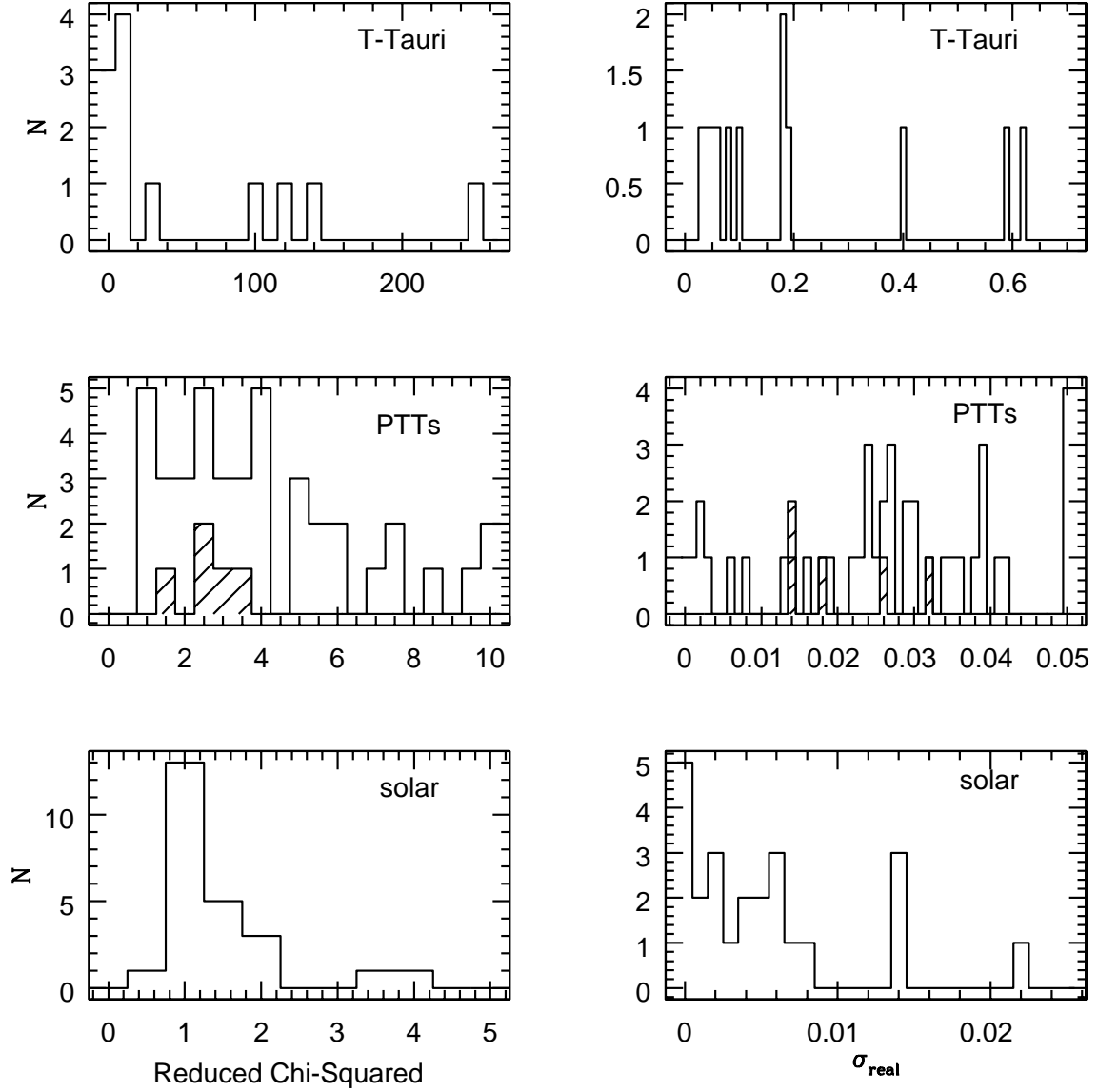
Fig. 8.— Histograms for χ^2_ν and real dispersions (σ_{real}) for *HIPPARCOS* V-magnitude variability. We have presented them in order of theoretically decreasing variability from the top down (i.e. TTs have the highest amount of irregular variability and solar analogs the lowest). The post T Tauri plot includes the 5 candidates we identify (shaded histogram) and a sample of 41 post T Tauri stars identified from the literature (unshaded histogram).
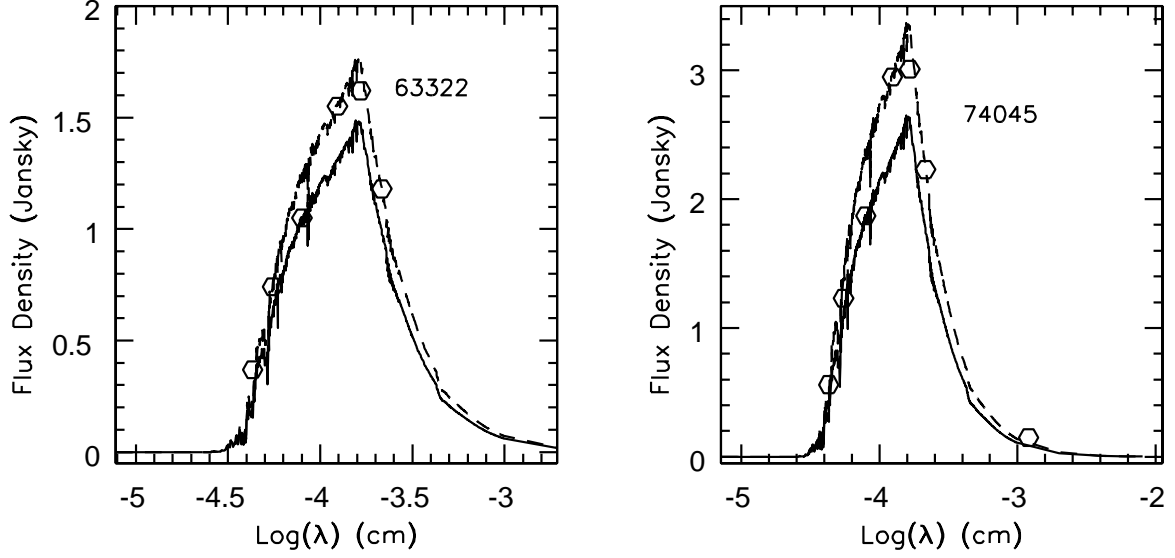
Fig. 9.— SEDs for the two post T Tauri stars (HIP 63322 and HIP 74045) that show an infrared excess in the J, H and K bands. The excess appears clearly when the kurucz fluxes are normalized to the Cousins I band (solid line). The excess, however, is essentially non-existant when kurucz fluxes are normalized to the 2MASS J band (dotted line). Errors are no greater than the size of the points.
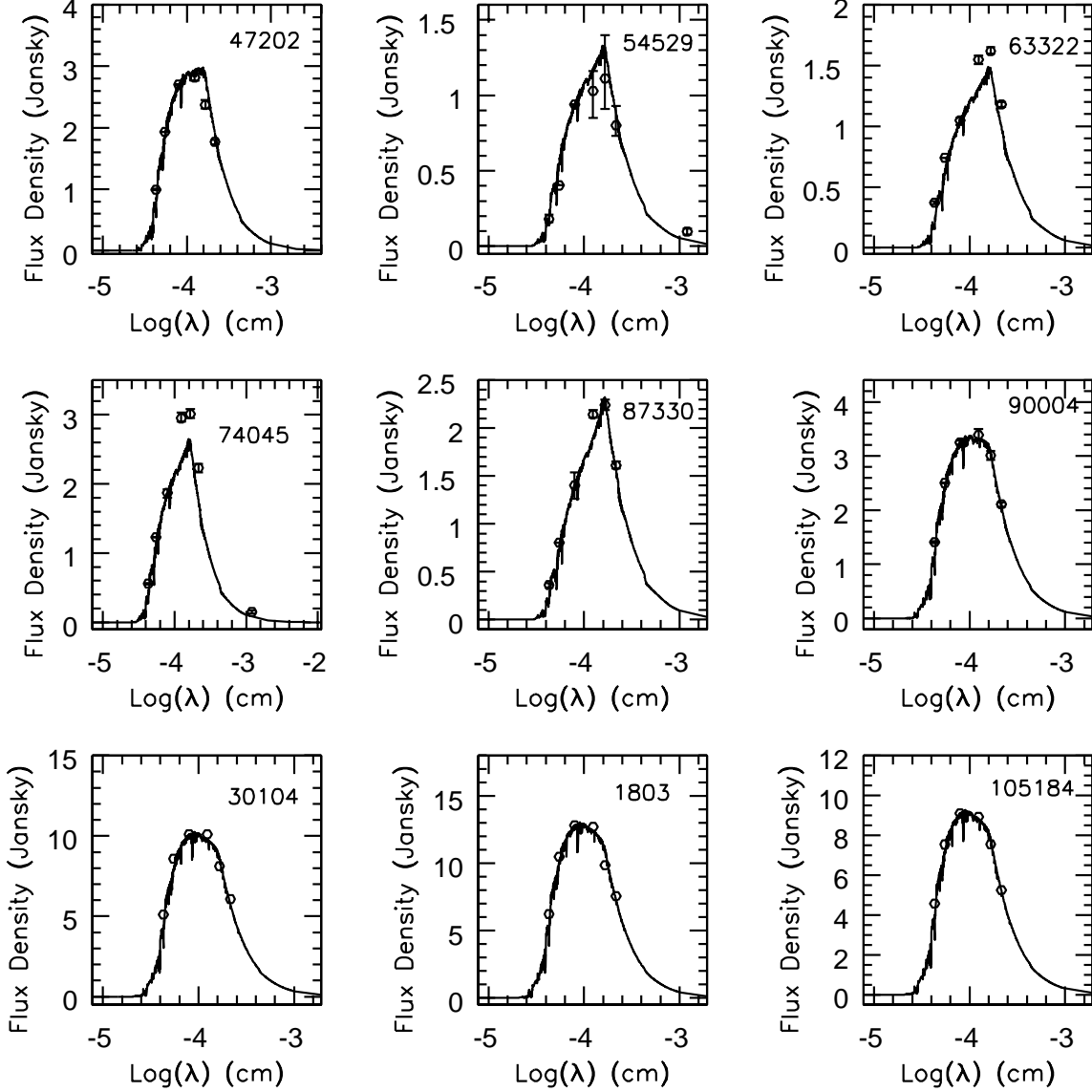
Fig. 10.— Kurucz model atmosphere flux curves and photometric data for a selection of our stars and for a sample of solar analogs. The top two rows are the stars in our sample and the bottom row provides curves for a sample of solar analogs. Each plot is labeled with the HIP number of the corresponding star and the Kurucz fluxes are normalized to the I$_{cousins}$ band. Note the apparent excess in the J and H and K bands in the post T Tauri stars (HIP 63322 and HIP 745045).
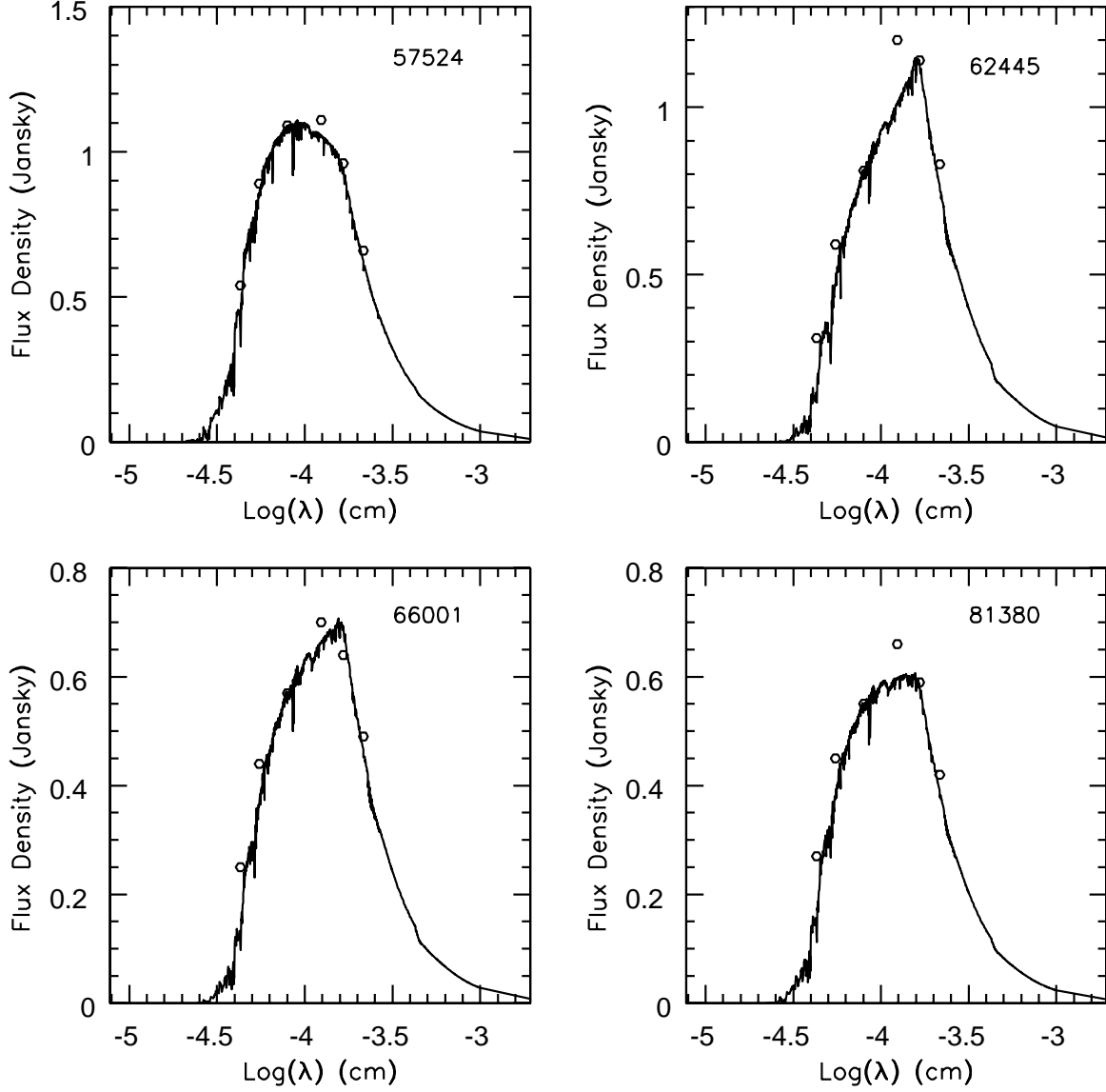
Fig. 11.— Kurucz model atmosphere flux curves and photometric data for a sample of post T Tauri stars taken from the literature. HIP numbers are given inside of each of the respective plots. We present this figure to demonstrate that post T Tauri stars appear to demonstrate many variations of excess. In some cases, the excesses are similar to those of our candidates (HIP 62445), although temperature differences may suggest a different conclusion (Fig.12).
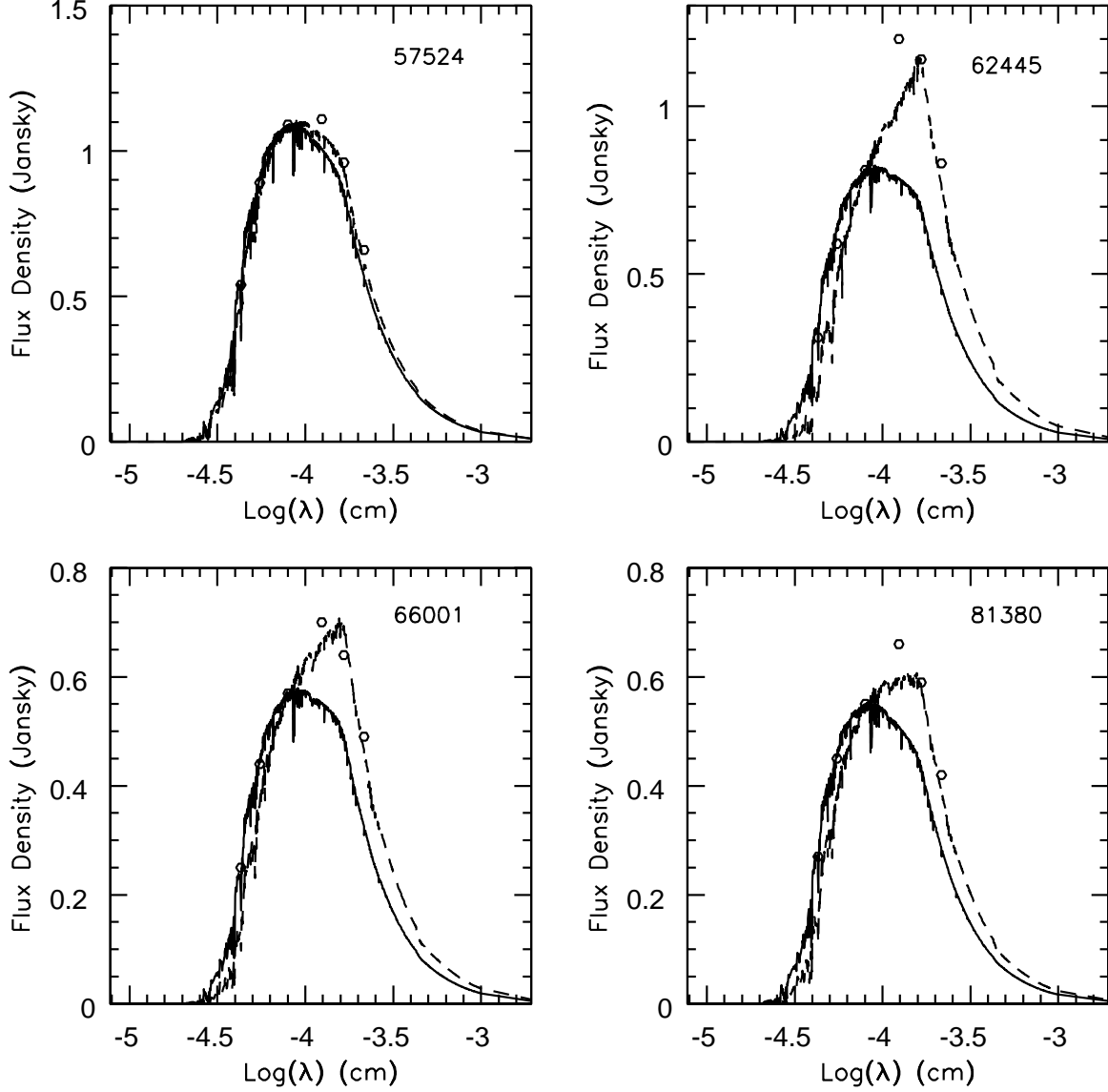
Fig. 12.— Comparison of kurucz model flux fits to photometric data for four literature post T Tauri aged stars (Mamajek et al. 2002). The solid curves are kurucz models for literature temperatures which were determined from calibrations to standard stars. The fit appears to improve when utilizing the photometric temperatures. We suggest that this demonstrates the usefulness of using photometric temperatures for the cooler stars represented by this sample.